Available online at www.sciencedirect.com
ScienceDirect
Ceramics International 35 (2009) 2077–2081
CERAMICS INTERNATIONAL
www.elsevier.com/locate/ceramint

Short communication

Synthesis of YAG powders by the co-precipitation method

Yongming Zhang *, Hongming Yu

School of Materials Science and Engineering, Shenyang Institute of Chemical Technology, Shenyang 110142, China

Received 27 March 2008; received in revised form 29 July 2008; accepted 1 October 2008
Available online 21 October 2008

Abstract

YAG ($Y_3Al_5O_{12}$) powders have been prepared by co-precipitation technique in which NH_4HCO_3 is used as a precipitant and Y_2O_3, A1($(NO_3)_3{\cdot}9H_2O$—as raw materials. Two kinds of surfactant are added into the solution, i.e. Polyethylene glycol (PEG10000) as steric stabilizer and $(NH_4)_2SO_4$ as electrical stabilizer. The composition of YAG precursor, the phase formation process of YAG and the properties of the powders were investigated by means of differential scanning calorimetry and thermogravimetry analysis (DSC–TG), X-ray diffraction (XRD), Fourier transformation infrared spectroscopy (FT-IR) and Scanning electron microscopy (SEM). The results of XRD show that phase YAG crystallite can be obtained as precursors when heated at 900 °C for 2 h. The powders loosely dispersed with narrow size distribution and spherical shapes could be observed by SEM. It has been found that the presence of PEG and $(NH_4)_2SO_4$ is beneficial for the dispersion of the resulting YAG powder. In the presence of surfactants, the synthesized product consists of highly dispersed nano-sized particles.

Keywords: Co-precipitation; YAG; Precursor powder; Dispersion; Surfactant

1. Introduction

Yttrium aluminum garnet (YAG) with the chemical composition $Y_3Al_5O_{12}$ is an important advanced optical material. Owing to the relatively stable lattice structure and large thermal conductivity [1], it is used as host for an important solid-state laser material in luminescence systems and window materials for a variety of lamps [2–4]. YAG also has great potential application as a high-temperature engineering material because of its better high-temperature strength as well as superior creep resistance [5–6]. In addition, YAG is a promising fibre material for the preparation of ceramic composites [7–9]. Translucent YAG doped with rare-earth ions (Nd: YAG) ceramics is a promising material for large-size solid-state lasers, as a substitute for single-crystal YAG because of its excellent laser performance, low cost, short preparation period, and other characteristics. YAG powders doped with transition and rare-earth metal elements can be used as ultra-short afterglow phosphors for cathode ray tubes and high-resolution displays [10]. In recent years, many efforts have been made for synthesizing YAG transparent ceramics for solid-state laser applications [11–12].

The powders with pure YAG phase are usually synthesized by conventional solid-state reaction method with Y_2O_3 and Al_2O_3 as raw materials. However, this method has some unavoidable disadvantages, such as high temperature, agglomerate particles, impurities due to the flux introduced and so on. The grinding process is necessary to obtain small particles. The extensive ball milling leads to possible contamination and degeneration of luminescent property [13]. In recent years, with the development of science and technology in the field of materials, a number of wet chemical synthesis methods have been developed and successfully used for the preparation of nano-sized powders. Their properties can be easily modified by changing the conditions during synthesis process [14]. These methods include sol–gel processing [15], metal-organic preceramic processing [16], hydrothermal synthesis [17] and co-precipitation methods [18]. These chemical processes achieve symmetrical mixing on the molecular level, lowering the crystallization temperature. Although the sol–gel method has some advantages, e.g. low-temperature synthesis, possible formation of powders with uniform grain morphology and achievement of homogeneous multi-component films [19], and has been successfully used to obtain undoped [20] and

* Corresponding author at: School of Material Science and Engineering, Shenyang Institute of Chemical Technology, Shenyang, 110142, No.11 Street, Economic and Technological Development Zone Shenyang, China.
Tel.: +86 24 89383326 fax: +86 24 89388153.
E-mail address: zymciom@126.com (Y. Zhang).

0272-8842/$34.00
doi:10.1016/j.ceramint.2008.10.002

rare-earth doped YAG phosphors, it has some disadvantages, such as hard controlling the pH, expensive starting materials and long-reaction time, all of which have limited its mass production. The hydrothermal and solvothermal synthesis of YAG powder can avoid the above-mentioned problems. However, hydrothermal synthesis requires complicated and expensive facilities due to the higher operating temperature and pressure (>400 °C, >30 MPa). Compared with these methods, co-precipitation is one of the most promising techniques because of precursor powders can be prepared on a large scale in water rather than in organic chemicals without using special apparatus. Nanosized YAG powder has been synthesized by the co-precipitation method, but the dispersion of the powder is not ideal. In order to achieve polycrystalline YAG ceramics with high density and high transparency, highly dispersed ultra-fine YAG powder is necessary .In this work, appropriate surfactants were used to control the dispersion of the YAG powder. The ammonium hydrogen carbonate (hereafter referred to as AHC) was used to synthesize YAG powders from a mixed solution of aluminum and yttrium nitrates via co-precipitation, in which polyethylene glycol (PEG10000) was used as steric stabilizer and $(NH_4)_2SO_4$ was used as electric stabilizer to obtain dispersed YAG cubic crystal phase with narrow particle size distribution and spherical shapes.

2. Experiment

The $Y(NO_3)_3$ was prepared by dissolving Y_2O_3 (99.99%, Zhujiang Rare-Earth Limited) in diluted nitric acid (HNO_3) followed by evaporating the excess acid and cooling to room temperature, and then distilled water was added. The $Al(NO_3)_3$ solution was obtained by dissolving $Al(NO_3)_3{\cdot}9H_2O$ (A.R., Tianjin Fine Chemicals) in deionized water. The concentrations of $Y(NO_3)_3$ solution and $Al(NO_3)_3$ solution were both 0.1 M. The AHC as precipitant is of analytical grade. PEG and $(NH_4)_2SO_4$ are both of analytical grade as the dispersant.

The nitrate solutions with molar ratio of 3:5 for Y^{3+}: Al^{3+} were mixed in a container and then 1 wt % disperser (PEG10000) and appropriately proportional $(NH_4)_2SO_4$ were added to the mixture and kept stirring. Then the mixtures were added drop-wise into the precipitant solution (ACH) at a speed of 2 ml per minute and under vigorous stirring at room temperature. The final pH of the suspensions was 8. The precipitated slurry was aged for 24 h to make the reaction sufficient, and then the suspensions were ltered and washed repeatedly with deionized water and ethanol to remove residual ammonia and nitric ions. After washing, the resulting product was dried at 80 °C for 10 h, and then the loose YAG precursors were obtained. Finally the YAG precursors were calcined in air at 800, 900, 1000 and 1100 °C for 2 h.

The thermal decomposition and/or crystallization behaviors was studied with the differential scanning calorimetry and thermogravimetry analysis (DSC–TG) at a heating rate of 10 °C per minute up to 1000 °C in air. The phase identification was performed by using a conventional D/max X-ray diffractometer (D8 Advance, Bruker, Germany) with CuKa radiation (λ = 1.54056 Å). The morphology of the powders annealed at 1100 °C for 2 h after being ultrasonically dispersed in ethanol was observed by SEM (JSM-6360LV, JEOM, Japan). The compositions of the precipitates were investigated by the Fourier transformation infrared spectroscope (FT-IR, PerkinElmer Company, Spectrum one).

3. Results and discussion

3.1. The effect of precipitate agent

In this work, ACH were used as precipitating agents. The precipitation processes were made by the reverse-strike method (adding the mixed salt solution to the precipitant solution). For the salt solution rich in cation, this method has the advantages of higher cation homogeneity in the materials.

For the ACH method, the chemical reactions of AHC hydrolysis are [21]:

$$NH_4HCO_3 + H_2O \rightarrow NH_4OH + H_2CO_3$$

$$H_2CO_3 \rightarrow H^+ + HCO_3^-$$

$$HCO_3^- \rightarrow H^+ + CO_3^{2-}$$

Thus, Al^{3+} may precipitate as AlOOH or $NH_4Al(OH)_2CO_3$, but as for the Y^{3+}, they may most likely precipitate as normal carbonate of $[Y_2(CO_3)_3{\cdot}nH_2O(n = 2,3)]$. This result is in agreement with the IR analysis of the YAG powder precursor. Thus it is certain that the YAG powder precursor produced by the ACH method is the compound carbonate which has the lower decomposition temperature.

It is important to keep a constant pH value by adding excess precipitating agent. If pH value varies too much, a segregation of Y^{3+} and Al^{3+} could happen. This will make the ratio of Y^{3+} and Al^{3+} deviate from 3:5 in local areas and, thus, some secondary phases could appear in the calcined powder.

3.2. The effect of surfactant

In order to avoid hard agglomeration of the precursors, PEG and $(NH_4)_2SO_4$ were added as steric stabilizer and electrical stabilizer during the precipitation process. PEG($H(OCH_2–CH_2)OH$) is a non-ionic dispersing agent with hydroxyls and ether groups. Metal ions (Y^{3+} and Al^{3+}) bond the oxygen atoms in the C–O–C chains, and can greatly inhibit agglomeration of cation. Especially, PEG can form a nearly spherical micelle on the precipitates ($NH_4Al(OH)_2CO_3$, AlOOH and $Y_2(CO_3)_3{\cdot}nH_2O$) by strong hydrogen bonds. The precipitates will be wrapped in the middle of the micelle during the reaction. Because of electrification of the polymer molecular surface, the micelles repel each other and avoid agglomeration of the precipitates in the solution. Also, the long-chain polymer can prevent adjacent arrangement of the precipitates due to Brownian motion. Finally, the expulsion of free water will cause shrinkage of the capillary channels during the drying process, which causes the precipitates to make intimate contact and so a strong chemical bond can be formed between them. After substitution of the polymer layer for free water on the surface of the precipitates,

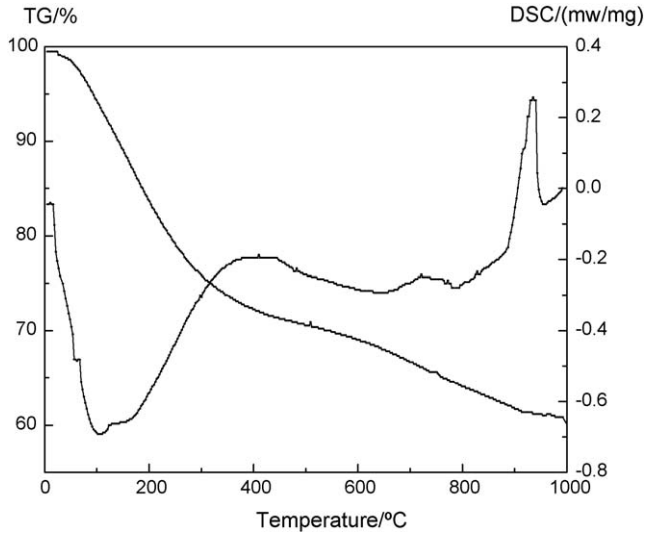

Fig. 1. TG–DSC curves of precursor powders.

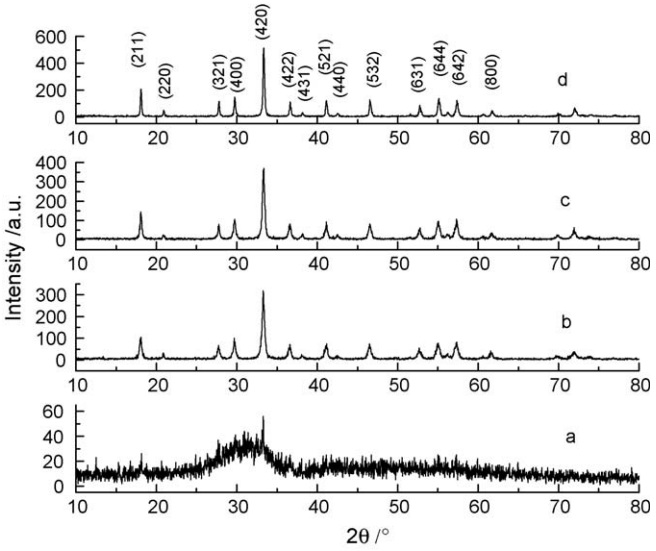

Fig. 2. XRD diffraction patterns of YAG precursor powders calcined at different temperatures: (a) 800 °C, (b) 900 °C, (c) 1000 °C, and (d) 1100 °C).

hard agglomeration caused by chemical bonding during the drying process is avoided. $(NH_4)_2SO_4$ was used as an electrical stabilizer agent during the reaction. Its function is to increase the ζ potential of precipitates in order to improve the repel of grain.

3.3. TG–DSC analysis

Fig. 1 shows the TG–DSC curves of precursor powder with a heating rate of 10 °C/min. The TG curve indicates the overall weight loss of approximately 38.9%. The 16.2% weight loss below 200 °C is caused by dehydration of physically adsorbed water and ethanol. The 17.5% weight lose between 200–800 °C is brought by the decomposition of carbonates and combustion of organic groups in the precursor powders. The 5.2% weight loss between 800–1000 °C is resulted in by decomposition of sulfates in the precursor powders. DSC curve consists of three endothermic peaks followed by an exothermic peak. The 120 °C endo-peak can be explained by the removal of physically adsorbed water and ethanol. The 660 °C endo-peak is caused by the decomposition of carbonates and oxidation of organic materials accompanied by great amounts of CO_2 and water vapor emitted, and 800 °C endo-peak is due to the decomposition of sulfates in the precursor powders accompanied by the SO_2 emitted. An exothermic peak at 935 °C can be attributed to crystallization and crystal growth of YAG. When the temperature is above 1000 °C, there are no changes in TG and DSC curves which show that the precursor powders completely transform to YAG cubic crystal phase. The XRD patterns (see Fig. 2) show that the crystallization of YAG began below the temperature, because the exothermic peak in the DSC curve often lags after the crystallization.

3.4. XRD analysis

The XRD patterns of the YAG precursor powders calcined between 800 and 1100 °C are shown in Fig. 2. No obvious diffraction peaks are observed when the particles were heated at 800 °C (see Fig. 2a). It can be concluded that the powder is amorphous below this temperature. With increasing in the calcination temperature, strong cubic-YAG diffraction peaks can be observed for the powder prepared at 900 °C in the XRD pattern shown in Fig. 2b. The YAG cubic crystalline phase is identified by the JCPDS# 33–40. Further heat treatment in the range of 900–1100 °C leads to the YAG diffraction peak intensity increased but no change in phase composition could be found. XRD spectra illustrated that YAG has completely been formed at a lower temperature (900 °C) without any other intermediate phase observed.

The line width of X-ray diffraction peaks gives us the information about crystallite size. The average crystallite size of the powder heated to different temperatures was determined from the line broadening observed for the peak

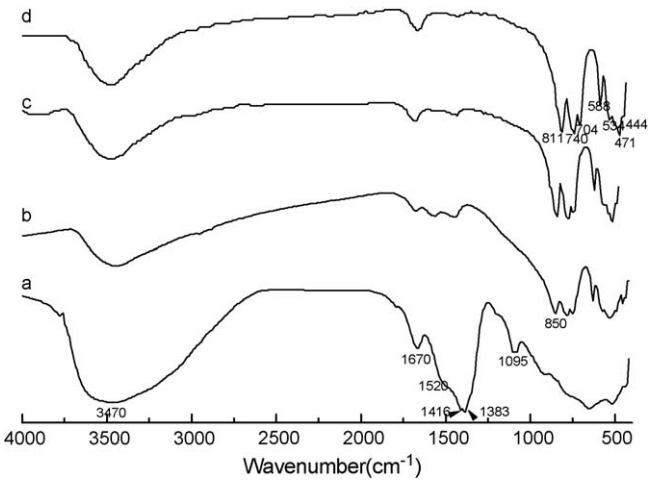

Fig. 3. FT-IR spectra of samples heat-treated at different temperatures: (a) precursor, (b) 800 °C, (c) 900 °C, and (d) 1000 °C.

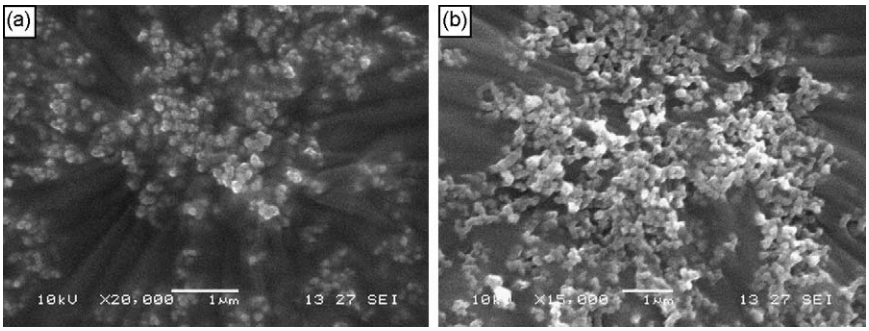

Fig. 4. SEM micrographs of YAG precursor powders heat-treated at 1100 °C for 2 h (a) at the presence of surfactants, and (b) without surfactants.

corresponding to the (420) reflection using the Scherrer's formula:

$$D = \frac{0.89\lambda}{\beta\cos\theta}$$

where D is the average crystallite size (Å), λ is the wavelength of X-ray used (1.54 Å), θ is the angle of diffraction (16.7° in this case), β is full widths (in radian) at half maximum observed for the sample. The average sizes of nanocrystallites were determined from width of diffraction lines according to Scherrer's formula to be approximately 72 nm (1000 °C, 2 h) and 78 nm (1100 °C, 2 h).

3.5. FT-IR analysis

Fig. 3 shows the IR spectra of the samples heated at various temperatures. The broad peak of 3470 cm^{-1} may result from the stretching vibrations of O–H bond including water and aluminum/yttrium hydroxyl groups. The broad peak becomes weaker with the temperature increasing. The weaker absorption band at 1670 cm^{-1} is from the bending vibrations of O–H bond. It is also caused by the absorption of H_2O in air. There are no significant changes in the FT-IR spectra with further increase in calcining temperature. The peak at about 1520 cm^{-1} can be attributed to NH_4^+ in the bond-stretching mode. Absorption bands at 1416 and 850 cm^{-1} may be caused by the absorption of CO_2 in the synthesized powder. The peak at about 1383 cm^{-1} is associated with the bond of N–O. When the heat-treated temperature increases, the peak becomes weaker and is almost not detected at 800 °C because of the decomposition of NO_3^{2-}. Other peak of 1095 cm^{-1} attributes to vibrations of the SO_4^{2-}. Thus, it is certain that precursor is Y^{3+} and Al^{3+} compound of carbonate and nitrate. When the temperature increased to 900 °C, the FT-IR spectrum of the YAG sample exhibited well defined peaks at 811, 740 cm^{-1} due to stretching vibrations of the AlO_6 octahedra and, also, showed absorption peaks at 471 and 444 cm^{-1} associated with the stretching of AlO_4 tetrahedra, while the peaks at about 704, 588 and 534 cm^{-1} represent the characteristics of Y-O metal–oxygen vibrations, all of which matched with the reported data for a well crystallized YAG [22]. These characteristic peaks appear at around 900 °C and become much sharper with the increasing firing temperature. These results indicating the decomposition of starting organics and the appearance of YAG fingerprints are in agreement with the thermal analysis and XRD as previous discussion.

3.6. SEM analysis

Fig. 4 shows the SEM morphologies of the YAG powders calcined at 1100 °C for 2 h. From Fig. 4a we can clearly see that well-dispersed YAG powder was synthesized in the presence of surfactants except for a few agglomerations of several particles. It can be noted that the grain size of YAG heat-treated at 1100 °C is about 70 nm .The grain sizes agree with the results of Scherrer's formula. By contrast, powder prepared in the absence of surfactants is filled with hard particle agglomerations as shown in Fig. 4b. This result can be understood by considering that a polymer molecule, especially SO_4^{2-} adsorbed on the surface of a precursor has a higher decomposition temperature, and its continued existence at a relatively high temperature may reduce the diffusion of elements between particles that contribute to better dispersion of the powder. In addition, SO_4^{2-} promoted the ζ potential of precipitant surface formed the stabilizing Stern layer, leading to stronger repulsion among particles and releasing agglomeration, too.

4. Conclusion

Highly dispersed YAG powder was synthesized by using the co-precipitation method with ammonium hydrogen carbonate as precipitant, and two kinds of surfactant, i.e. polyethylene glycol (PEG10000) as steric stabilizer and $(NH_4)_2SO_4$ as electrical stabilizer. It has been found that the presence of the PEG and $(NH_4)_2SO_4$ is beneficial for producing dispersion of the resulting YAG powder. XRD results showed that the precursor had converted directly to pure YAG at about 900 °C without any intermediates. YAG powder calcined at 1100 °C for 2 h is well dispersed with an average crystallite size of 78 nm. The powder produced will thus be more desirable for compacting and sintering YAG transparent ceramics.

Acknowledgements

This work was supported by the Liaoning Provincial Office of Education (Grant No.2005319). Authors are grateful to the

SEM section, XRD section and FTIR section for their constant support. We also cordially thank Prof. Li Yanhong for her helpful discussion.

References

[1] B. Vaidhyanathan, J.G.P. Binner, Microwave assisted synthesis of nanocrystalline YAG, J. Mater. Sci. 41 (2006) 5954–5957.
[2] J.T. Vega-Duran, O. Barbosa-Garcia, L.A. Diaz-Torres, M.A. Meneses-Nava, Effects of energy back transfer on the luminescence of Yb and Er ions in YAG, Appl. Phys. Lett. 76 (15) (2000) 2032–2034.
[3] D. Jun, D. Peizhen, X. Jun, The growth of Cr^{4+}, Yb3^{+}: yttrium aluminum garnet (YAG) crystal and its absorption spectra properties, J. Cryst. Growth 203 (1999) 163–167.
[4] A. Ikesue, K. Yoshida, K. Kamata, Effects of Nd concentration on optical characteristics of polycrystalline Nd: YAG ceramics laser, J. Am. Ceram. Soc. 79 (7) (1996) 1921–1926.
[5] W.R. Blumenthal, D.S. Phillips, High-temperature deformation of single-crystal yttrium-aluminum garnet (YAG), J. Am. Ceram. Soc. 79 (4) (1996) 1047–1052.
[6] K. Keller, T. Mah, T.A. Part hasarathy, Processing and mechanical properties of polycrystalline $Y_3Al_5O_{12}$ (yttrium aluminum garnet), Ceram. Eng. Sci. Proc. 11 (1990) 1122–1133.
[7] G.S. Corman, Creep of yttrium aluminium garnet single crystals, J. Mater. Sci. Lett. 12 (6) (1993) 379–382.
[8] T. Isobe, M. Omori, S. Uchida, T. Sato, T. Hirai, Consolidation of Al_2O_3-$Y_3Al_5O_{12}$ (YAG) eutectic powder prepared from induction-melted solid and strength at high temperature, J. Eur. Ceram. Soc. 22 (2002) 262l–2625.
[9] A. Kareiva, C.J. Harlan, D.B. MacQueen, R. Cook, A.R. Barron, Carboxylate-substituted alumoxanes as processable precursors to transition metal-aluminum and lanthanide-aluminum mixed-metal oxides: atomic scale mixing via a new transmetalation reaction, Chem. Mater. 8 (9) (1996) 233l–2340.
[10] Xudong Zhang, Hong Liu, Wen He, et al., Novel synthesis of YAG by solvothermal method, J. Cryst. Growth 275 (2005) e1913–e1917.
[11] A. Ikesue, I. Furusato, K. Kamata, Fabrication of polycrystal line, transparent YAG ceramics by a solid-state reaction method, J. Am. Ceram. Soc. 78 (1) (1995) 225–228.
[12] A. Ikesue, K. Kamata, K. Yoshida, Synthesis of (Nd^{3+}, Cr^{3+})-codoped YAG ceramics for high-efficiency solid-state lasers, J. Am. Ceram. Soc. 78 (9) (1995) 2545–2547.
[13] M. Li, Principles and synthesis of ceramic powder by means of wet chemical method, J. Chin. Ceram. Soc. 22 (1) (1994) 85–91.
[14] Q. Zhang, F. Saito, Mechanochemical solid reaction of yttrium oxide with alumina leading to the synthesis of yttrium aluminum garnet, Powder Technol. 129 (1) (2003) 86–91 (6).
[15] T. Tachiwaki, M. Yoshinaka, et al., Novel synthesis of $Y_3Al_5O_{12}$ (YAG) leading to transparent ceramics, Solid State Commun. 119 (2001) 603–606.
[16] Y. Liu, Z.F. Zhang, B. King, J. Halloran, R.M. Laine, Synthesis of yttrium aluminum garnet using isobutyrate precursors, J. Am. Ceram. Soc. 79 (1996) 385–389.
[17] Y. Hakuta, K. Seino, Haruo Ura, et al., Production of phosphor (YAG: Tb) fine particles by hydrothermal synthesis in supercritical water, J. Mater. Chem. 9 (1999) 2671–2674.
[18] M. Yada, M. Ohya, M. Machida, T. Kijima, Synthesis of porous yttrium aluminium oxide templated by dodecyl sulfate assemblies, Chem. Commun. (1998) 1941–1942.
[19] A. Potdevin, G. Chadeyron, D. Boyer, et al., Sol–gel elaboration and characterization of YAG: Tb^{3+} powdered phosphors, J. Mater. Sci. 41 (8) (2006) 2201–2209.
[20] R. Manalert, M.N. Rahaman, Sol–gel processing and sintering of yttrium aluminum garnet (YAG) powders, J. Mater. Sci. 31 (10) (1996) 3453–3458.
[21] Xia Li, Hong Liu, Jiyang Wang, et al., Preparation and properties of YAG nano-sized powder from different precipitating agent, Opt. Mater. 25 (4) (2004) 407–412.
[22] M. Panneerselvam, G.N. Subanna, K.J. Rao, Translucent yttrium aluminum garnet: microwave-assisted route to synthesis and processing, Mater. Res. Soc. 16 (10) (2001) 2773–2776.

Zhang Yongming (1964-), Ph.D, associate professor; research field: photoelectronic functional materials.